of binding these complex adsorbates strongly to very high surface densities, perhaps approaching that of a solid-like organic phase of low dimensionality.

We and others will detail additional properties of this intriguing chemisorption system and show relevant applications to the study of model organic surfaces, interfaces, and their properties in future publications.

Acknowledgment. We wish to express our appreciation to Professor George M. Whitesides and his co-workers, especially Dr. B. Troughton, Dr. S. R. Holmes-Farley, and C. Bain, for many useful and informative discussions. We are especially indebted to D. Allara, with whom much collaborative work on this subject has been conducted. Helpful comments from C. Chidsey and E. Chandross are also acknowledged.

Molecular Structure and Magnetic Properties of a Novel Fe(III) Tetranuclear Complex Containing Oxo, Alkoxo, and Carbonato Bridges

Donald L. Jameson,[1a] Chuan-Liang Xie,[1b] David N. Hendrickson,*[1b] Joseph A. Potenza,*[1a] and Harvey J. Schugar*[1a]

Contribution from the Department of Chemistry, Rutgers, The State University of New Jersey, New Brunswick, New Jersey 08903, and the School of Chemical Sciences, University of Illinois, Urbana, Illinois 61801. *Received April 22, 1986*

Abstract: The crystal structure and magnetic properties of a novel antiferromagnetic Fe(III) complex that contains bridging carbonato, oxo, and alkoxo groups are reported. The complex (**1**) crystallizes as brown-green tablets in space group $P\bar{1}$ with a = 11.712 (4) Å, b = 12.914 (3) Å, c = 10.987 (3) Å, α = 94.03 (2)°, β = 116.00 (2)°, γ = 77.70 (2)°, Z = 1, d_{calcd} = 1.72 g/cm^3, and d_{obsd} = 1.71 (2) g/cm^3. Least-squares refinement of 3126 reflections having $F^2 > 2\sigma$ gave a conventional R factor of 0.085. The structure contains centrosymmetric tetranuclear complexes consisting of two binulcear $Fe_2L(O)(CO_3)$ units where L is the pentaanionic form of [(2-hydroxy-1,3-propanediyl)diimino]tetraacetic acid. The Fe(III) ions within the $Fe_2L(O)(CO_3)$ asymmetric unit have slightly different NO_5 distorted octahedral ligand donor sets in which the O-donors are supplied by two monodentate acetates, a bridging oxide, a bridging alkoxide, and one oxygen atom per Fe from the bridging bidentate carbonates. The bent Fe_2O(oxo) unit (136.4 (3)°) contains the shortest Fe–O bonds (1.828 (4), 1.830 (4) Å) in the structure. These are, however, among the longest reported for an oxo-bridged binuclear Fe(III) unit. The Fe–O bonds arising from the bridging carbonate group are equivalent (1.989 (4), 1.997 (4) Å) within experimental error. The Fe–O(alkoxo) bonds (2.040 (4), 2.066 (4) Å) are nearly equivalent and fall outside the range (1.93–2.01 Å) reported for various hydroxo- or alkoxo-bridged Fe(III) binuclear complexes. One lattice Na^+ ion, located on a center of symmetry, joins the tetranuclear anions to form infinite chains along [110]. The effective magnetic moment per Fe(III) in **I** varies gradually from 2.42 μ_B at 300 K to 0.36 μ_B at 15 K. Magnetically, the structure is most conveniently viewed as containing μ-oxo, μ-carbonato dimers linked by additional μ-alkoxo bridges. A molecular field model was used to approximate the case where intradimer magnetic coupling (J) of the oxo/carbonato binuclear unit is expected to dominate the relatively weaker interdimer coupling (J') expected from the two long alkoxo bridges. The experimental data were well fit with J = −63.4 cm^{-1}, J' = −11.2 cm^{-1}, g = 2.0, and TIP = 800 × 10^{-6} cgsu. The intradimer coupling constant is considerably smaller than the values reported (−90 to −120 cm^{-1}) for oxo-bridged Fe(III) binuclear complexes, and this may be attributed to the somewhat long Fe–O(oxo) bond distances observed in **1**. Structural reasons for this effect are discussed. In contrast, the J' value is typical of that found for hydroxy/alkoxy-bridged Fe(III) dimers.

Polynuclear systems with two or more Fe(III) ions bridged by oxygen donor ligands are pertinent to the inorganic and bioinorganic chemistry of ferric ion. The simplest and most thoroughly studied systems are binuclear complexes in which the Fe(III) ions are bridged by a single oxo or by two hydroxo or alkoxo bridges. The oxo-bridged binuclear complexes exhibit unusual electronic spectroscopic properties[2] along with appreciable antiferromagnetic exchange interactions which may be described by the $-2JS_1S_2$ exchange Hamiltonian with $S_1 = S_2 = 5/2$, $-J$ = 90 to 120 cm^{-1}, and g = 2.0. The magnitude of the antiferromagnetic interaction is surprisingly insensitive to the natures of the non-bridging ligands, Fe(III) coordination numbers, and Fe–O–Fe bridging angles.[3] The $Fe_2(OR)_2^{4+}$ binuclear systems (R = H, alkyl) are far more weakly coupled magnetically ($-J$ = 10 to 15 cm^{-1}) and exhibit electronic absorptions which are little changed from those of magnetically isolated Fe(III) monomers.[3,4] The oxo-bridged binuclear complexes are by far the most commonly observed of these two types. They seem to constitute a thermodynamic pit for numerous Fe(III)–ligand systems, and their appearance in the literature has continued without interruption since the first structural characterization in 1967.[5] Studies of binuclear Fe(III) complexes have been stimulated by reports that three metalloprotein systems contain (in their fully oxidized states) binuclear Fe(III) units, all of which seem to be the more common oxo-bridged type. The best characterized of these is the non-heme O_2 transport protein hemerythrin in which the Fe(III) ions additionally are bridged by the carboxylate side chains of glutamate and aspartate protein residues.[6,7] The non-bridging ligands include five histidine imidazoles and hydroperoxide.[8,9] Dissociation of

(1) (a) Rutgers University. (b) University of Illinois.
(2) Schugar, H. J.; Rossman, G. R.; Barraclough, C. G.; Gray, H. B. *J. Am. Chem. Soc.* **1972**, *94*, 2683.
(3) Thich, J. A.; Toby, B. H.; Powers, D. A.; Potenza, J. A.; Schugar, H. J. *Inorg. Chem.* **1981**, *20*, 3314.
(4) Chiari, B.; Piovesana, O.; Tarantelli, T.; Zanazzi, P. F. *Inorg. Chem.* **1984**, *23*, 3398.
(5) Lippard, S. J.; Schugar, H.; Walling, C. *Inorg. Chem.* **1967**, *6*, 1825.
(6) Stenkamp, R. E.; Sieker, L. C.; Jensen, L. H. *J. Am. Chem. Soc.* **1984**, *106*, 618.
(7) Scheriff, S.; Hendrickson, W. A.; Smith, J. L. *Life Chem. Rep.* **1983**, *Suppl. 1*, 305.
(8) Kurtz, D. M.; Shriver, D. F.; Klotz, I. M. *J. Am. Chem. Soc.* **1976**, *98*, 5033.

0002-7863/87/1509-0740$01.50/0

Table I. Results of Elemental Analyses for **1**

	"wet" analysis				"dry" analysis		
	I[a]	II[b]	III[c]	calcd[d]	I[a]	II[b]	calcd[e]
C	19.88	18.89	19.77	19.11	24.16	24.46	25.11
N	3.90	3.53	4.05	3.72	5.25	4.67	4.88
H	4.18	3.64	3.74	4.41	2.75	2.86	2.28
Na	8.99		8.91	9.15	11.27		12.02
Fe	15.54		15.75	14.81	20.78		19.46
Na/Fe	1.40		1.38	1.5	1.32		1.5
C/N	5.94	6.24	5.69	6.5	5.37	6.10	6.5

[a] Schwartzkopf Microanalytical Laboratory. [b] Robertson Laboratories, Inc. [c] Galbraith Laboratories, Inc. [d] Calculated for $Na_6Fe_4L_2(O)_2(CO_3)_2 \cdot 2OH_2O$, L = $C_{11}H_{13}N_2O_9$. [e] Calculated for $Na_6Fe_4L_2(O)_2(CO_3)_2$, L = $C_{11}H_{13}N_2O_9$.

the peroxide as O_2 yields a binuclear Fe(II) unit which remains coupled by the carboxylate bridges; recent spectroscopic studies have led to the suggestion that the ferrous ions additionally are coupled by a single hydroxo or oxo bridge.[10a,b] The peroxide group of the oxyhemerythrin may be displaced by several ligands to yield a variety of "methemerythrins".[11] The electronic spectroscopic features of these systems are duplicated remarkably well by model complexes of the type $LFe(O)(acetate)_2FeL$ where L = tris-1-pyrazolylborate or a 1,4,7-triazacyclononane,[12,13] and the chemical features of the models are proving to be interesting as well.[14,15] Less well characterized oxo-bridged Fe(III) units are thought to be present in ribonucleotide reductase of *E. coli*[16,17] and in the purple acid phosphatases isolated from pig allantoic fluid[18,19] and beef spleen.[20] There appear to be no known biological Fe(III) cluster units intermediate in size between the above binuclear complexes and the polymeric core of composition $[(FeO\cdot OH)_8\cdot OPO_3H_2]_n$ contained in the iron storage protein ferritin.[21] Consequently, there is some interest in establishing details pertaining to the polymerization of dimeric units. In the case of inorganic Fe(III) systems, the next higher cluster complexes are the trinuclear Fe_3O^{7+} species in which the Fe(III) ions additionally are bridged by carboxylate,[2] sulfate,[2,22] or phosphodiester groups.[23] These trinuclear complexes have been synthesized without the isolation of potentially precursor binuclear intermediates. Conversion of an Fe_2O^{4+} binuclear complex to a trinuclear complex of considerably different nature recently has been reported by Gorun and Lippard.[24] The surprising dynamics of electron exchange within mixed valence $Fe^{III}_2Fe^{II}$ clusters has been revealed in a series of reports from the Hendrickson group.[25] Conversion of a hydroxo/phenoxo-bridged Fe(III) binuclear complex into a tetranuclear complex in which each Fe(III) is linked to the other three by an oxo, hydroxo, and phenoxy bridge has been reported recently by Que and co-workers.[26a,b] Toftlund and co-workers recently have described a tetranuclear complex which consists of two well-separated μ-oxo-bis(μ-acetato)Fe^{III} units.[27] A tetranuclear complex of composition $Fe_4O_2(CF_3CO_2)_8(H_2O)_6$ has been described by Turte' and co-workers.[28] Other tetranuclear Fe(III) complexes are described in a recent review by Lippard.[29] Higher iron-containing clusters have also been prepared. Wieghardt and co-workers found that the 1,4,7-triazacyclononane $FeCl_3$ system at pH 9 in the absence of acetate yields a novel octanuclear Fe(III) complex with twelve hydroxobridges and two oxobridges.[30] Finally, Gorun and Lippard have recently reported an aggregate of composition $Fe_{11}O_6(OH)_6(O_2CPh)_{15}$.[31]

We report here the structural and detailed magnetic susceptibility studies of the title species, a novel tetranuclear Fe(III) complex containing two molecules of the pentaanionic form of the ligand [(2-hydroxy-1,3-propanediyl)diimino]tetraacetic acid. Potentiometric titration studies revealed that strong 2:1 Fe(III):ligand complexes could be prepared in solution.[32] The presence of open coordination sites on this 2:1 complex suggested that hydrolysis and condensation to higher aggregates could be achieved; this result has been realized.

Experimental Section

1. Preparation of $Na_6Fe_4L_2(O)_2(CO_3)_2\cdot\approx 2OH_2O$ ($Na_6(1)\cdot\approx 2OH_2O$, L = $O_9N_2C_{11}H_{13}$). This complex was prepared by the reaction of [(2-hydroxy-1,3-propanediyl)diimino]tetraacetic acid (LH_5, **2**, Sigma Chemical Co.) with an aqueous slurry of $Fe(OH)_3$ followed by the addition of $NaHCO_3$. The $Fe(OH)_3$ was prepared by treating 5.4 g (20 mmol) of $FeCl_3\cdot 6H_2O$ in 100 mL of H_2O with a solution of 2.4 g (60 mmol) of NaOH in 15 mL of H_2O, isolated by centrifugation, and freed of chloride by stirring with H_2O and recentrifuging (4×). A slurry of the purified $Fe(OH)_3$ in 100 mL of H_2O was reacted with 3.22 g (10 mmol) of **2** for 1 h at 70 °C. Solid $NaHCO_3$ (1.68 g, 20 mmol) was added slowly (effervesence) to the resulting yellow solution; the pH increased from 1.5 to 8.0 and the color changed to brown-green. After the solution was stirred for 12 h, the pH increased to 8.5. The solution was filtered through a fine frit and reduced in volume to 50 mL by rotoevaporation. Small, brown-green, tablet-shaped crystals deposited over a 3-day period from a mixture of 15 mL of the above concentrate and 50 mL of methoxyethanol that was placed in a dessicator containing $CaCl_2$. The crystals were collected by filtration and dried briefly by blotting (yield ≈50%). The crystals crack upon exposure to air for more than a few minutes or to water-miscible organic solvents, but they are stable for at least several hours under mineral oil. Careful microscopic examination of the product established that a single crystalline phase was obtained.

To help determine the empirical formula of these highly effluorescent crystals, several elemental analyses (Table I) were performed. Crystals were either blotted dry ("wet" analysis) or blotted dry and then heated at 140 °C for 15 h to remove lattice water ("dry" analysis). Crystallo-

(9) Dunn, J. B. R.; Shriver, D. F.; Klotz, I. M. *Proc. Natl. Acad. Sci. U.S.A.* **1973**, *70*, 2582.
(10) (a) Reem, R. C.; Solomon, E. I. *J. Am. Chem. Soc.* **1984**, *106*, 8323; (b) Shiemke, A. K.; Loehr, T. M.; Sanders-Loehr, J. *J. Am. Chem. Soc.* **1986**, *108*, 2437 and references cited therein.
(11) Sanders-Loehr, J.; Loehr, T. M. *Adv. Inorg. Biochem.* **1979**, *1*, 235. Klotz, I. M.; Kurtz, D. M. *Acc. Chem. Res.* **1984**, *17*, 16.
(12) Armstrong, W. H.; Spool, A.; Papaefthymiou, G. C.; Frankel, R. B.; Lippard, S. J. *J. Am. Chem. Soc.* **1984**, *106*, 3653.
(13) Wieghardt, K.; Pohl, K.; Gebert, W. *Angew. Chem., Int. Ed. Engl.* **1983**, *22*, 727.
(14) Wieghardt, K.; Pohl, K.; Ventur, D. *Angew. Chem., Int. Ed. Engl.* **1985**, *24*, 392.
(15) Armstrong, W. H.; Lippard, S. J. *J. Am. Chem. Soc.* **1984**, *106*, 4632.
(16) Reichard, P.; Ehrenberg, A. *Science* **1983**, *221*, 514.
(17) Sjoberg, B.-M.; Graslund, A. *Adv. Inorg. Biochem.* **1983**, *5*, 87.
(18) Antanaitis, B. C.; Aisen, P.; Lilienthal, H. R. *J. Biol. Chem.* **1983**, *258*, 3166.
(19) Sinn, E.; O'Connor, C. J.; de Jersey, J.; Zerner, B. *Inorg. Chim. Acta* **1983**, *78*, L13.
(20) Davis, J. C.; Averill, B. A. *Proc. Natl. Acad. Sci. U.S.A.* **1982**, *79*, 4623.
(21) Theil, E. C. *Adv. Inorg. Biochem.* **1983**, *5*, 1.
(22) Giacovazzo, C.; Scordari, F.; Menchetti, S. *Acta Crystallogr., Sect. B* **1975**, *B31*, 2171.
(23) Armstrong, W. H.; Lippard, S. J. *J. Am. Chem. Soc.* **1985**, *107*, 3730.
(24) Gorun, S. M.; Lippard, S. J. *J. Am. Chem. Soc.* **1985**, *107*, 4568.
(25) Oh, S. M.; Hendrickson, D. N.; Hassett, K. L.; Davis, R. E. *J. Am. Chem. Soc.* **1985**, *107*, 8009.
(26) (a) Murch, B. P.; Boyle, P. D.; Que, L., Jr. *J. Am. Chem. Soc.* **1985**, *107*, 6728. (b) Que, L., Jr.; Murch, B. P.; Bradley, F. C. *Abstracts of Papers*, National Meeting of the American Chemical Society, Anaheim, CA; American Chemical Society: Washington, DC, 1986; INOR 253.
(27) Toftlund, H.; Murrary, K. S.; Zwack, P. R.; Taylor, L. F.; Anderson, O. P. *J. Chem. Soc., Chem. Commun.* **1986**, 191.
(28) Turte', K. I.; Bobkova, S. A.; Kuyavskaya, B. Ya.; Ivleva, I. N.; Veksel'man, M. E. *Koord. Khim.* **1985**, *11*, 1106.
(29) Lippard, S. J. *Chem. Br.* **1986**, 222.
(30) Wieghardt, K.; Pohl, K.; Jibril, I.; Huttner, G. *Angew. Chem., Int. Ed. Engl.* **1984**, *23*, 77.
(31) Gorun, S. M.; Lippard, S. J. *Nature (London)* **1986**, *319*, 666.
(32) Klausen, K. S.; Ruud, O. E. *Anal. Chim. Acta* **1971**, *57*, 351.

Table II. Crystal and Refinement Data for $Na_6Fe_4(O_9N_2C_{11}H_{13})_2(O)_2(CO_3)_2 \cdot 2OH_2O$

formula	$Fe_4Na_6O_{46}N_4C_{24}H_{66}$
fw	1508.117
a, Å	11.712 (4)
b, Å	12.914 (3)
c, Å	10.987 (3)
α, deg	94.03 (2)
β, deg	116.00 (2)
γ, deg	77.70 (2)
V, Å^3	1458.8 (14)
space group	$P\bar{1}$
Z	1
no. of refs used to determine cell constants	25 ($13.3 \leq \theta \leq 18.9°$)
d_{calcd}, g/cm^3	1.72
d_{obsd}, g/cm^3	1.71 (2)
λ(Mo Kα), Å	0.71073
monochromator	graphite
linear abs coeff, cm^{-1}	11.3
crystal dimens, mm	0.34 × 0.40 × 0.08
rel trans factor range	$0.78 < T < 1$
diffractometer	Enraf–Nonius CAD-4
data collection method	θ–2θ
2θ range, deg	$2 \leq 2\theta \leq 50$
temp, K	298 (1)
scan range, deg	$0.90 + 0.35 \tan \theta$
weighting scheme	$w = 4(F_o)^2/[\sigma(F_o)^2]^2$ [a]
no. of std reflcns	3
% variation in std intens	±2.8
no. of unique data collected	5024
no. of data used in refinement	3126 ($F_o^2 \geq 2\sigma(F_o^2)$)
data:parameter ratio	8.7
final G.O.F.[b]	2.67
final R_F[c]	0.085
final R_{wF}[d]	0.099
systematic absences obsd	none
final largest shift/esd	0.03
highest peak in final diff. map, e/Å^3	1.09

[a] $[\sigma(F_o)^2]^2 = [S^2(C + R^2B) + (rF_o^2)^2]/(Lp)^2$, where S is the scan rate, C is the total integrated peak count, R is the ratio of scan to background counting time, B is the total background count, and r is a factor introduced to downweight intense reflections. For the present structure, $r = 0.04$. [b] Error in an observation of unit weight, equal to $[\sum w(|F_o| - |F_c|)^2/(NO - NV)]^{1/2}$ where NO is the number of observations and NV is the number of variables in the least-squares refinement. [c] $R_F = \sum||F_o| - |F_c||/\sum|F_o|$. [d] $R_{wF} = [\sum w(|F_o| - |F_c|)^2/\sum wF_o^2]^{1/2}$.

graphic analysis (see below) clearly indicated a tetranuclear iron complex containing two ligands L = $C_{11}H_{13}N_2O_9$ and two bridging O atoms, but it could not distinguish between bridging carbonate (e.g., $Na_6Fe_4L_2O_2(CO_3)_2$) or bicarbonate ($Na_4Fe_4L_2O_2(HCO_3)_2$) groups. The Na/Fe ratio is sensitive to the amount of bicarbonate, the C/N ratio is not, and both ratios are independent of the amount of lattice water present. From Table I, the observed Na/Fe ratio (av 1.37) is consistent with predominantly (92%) carbonato bridging; this, the scatter in the C/N ratio and the deviation of the average value (5.87) from the expected value (6.5) lead us to conclude that, within experimental error, the elemental analyses are consistent with carbonate bridging and provide little evidence for bicarbonate bridging.

2. X-ray Diffraction Studies. A well-formed tabular crystal was mounted inside a glass capillary with epoxy glue and prevented from dehydrating by a small amount of mother liquor well removed from the crystal. All diffraction measurements were made with an Enraf-Nonius CAD-4 diffractometer and graphite-monochromated Mo Kα radiation. The Enraf-Nonius Structure Determination Package[33] was used for data collection, data processing, and structure solution. Diffractometer examination of the reciprocal lattice revealed a triclinic system with no systematic absences. The density of the crystals was measured with use of a gradient prepared from ethylene bromide and heptane. To minimize errors arising from crystal dehydration, measurements were made on crystals that were blotted dry and studied immediately. The density increased with time from a value of 1.71 (fresh) to 1.83 g/cm^3 (partially dehydrated). Crystal data and additional details of data collection and refinement are presented in Table II. Intensity data were collected and corrected for decay, absorption (empirical), and Lp effects.

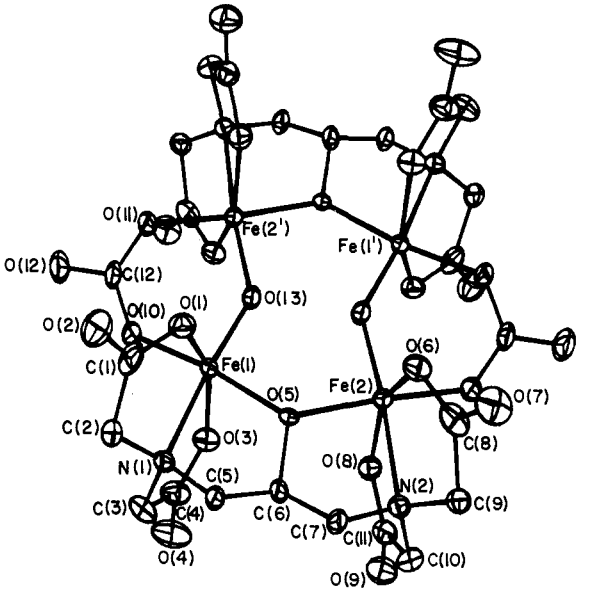

Figure 1. ORTEP view of the tetranuclear $Fe_4L_2(O)_2(CO_3)_2^{6-}$ anion **1** showing the atom numbering scheme. H atoms have been omitted for clarity.

The structure was solved by direct methods[34] and refined on F with full-matrix least-squares techniques. An E map, based upon 450 phases ($|E| > 1.74$) from the starting set with the highest combined figure of merit revealed coordinates for both unique Fe atoms and for part of the ligand L. The remaining ligand non-H atoms were located from successive difference Fourier maps, and it was clear at this point that the structure contained centrosymmetric, tetranuclear Fe units bridged by the ligand alkoxo groups, oxide ions, and either carbonate or bicarbonate groups. From the elemental analysis results we assumed that the empirical formula was best represented as the Na salt of the carbonato-bridged tetranuclear complex with approximately 20 H_2O lattice molecules required by the observed density.

Location and identification of these lattice species proved to be difficult. A difference map based on the coordinates of the tetranuclear complex revealed one Na, five water O sites, and many smaller peaks which were assumed to be disordered Na or H_2O species. Numerous structure factor, difference Fourier calculations were performed in an attempt to determine crystallographically the number of lattice species. Atoms were assigned as Na or O(H_2O) on the basis of geometrical considerations, while atom multipliers were set in accordance with observed electron densities and to avoid chemical impossibilities. In this way, a total of 4.6 Na ions and 19.9 lattice O atoms were added to the unit cell. In the asymmetric unit (half the unit cell), this corresponded to 7 Na sites and 14 O sites either totally or partially occupied (Table III).

All atoms in the tetranuclear complex as well as the four lattice species on completely occupied sites were refined anisotropically; lattice species on partially occupied sites were refined isotropically with their atom multipliers held constant. Ligand H atoms were added at calculated positions assuming idealized bond geometry and C–H and N–H distances of 0.95 and 0.87 Å, respectively.[35] No attempt was made to locate H_2O H atoms. H atom temperature factors were set according to $B_H = B_N + 1$ where N is the atom bonded to H. Hydrogen atom parameters were not refined. Several cycles of refinement led to convergence with $R_F = 0.085$ and $R_{wF} = 0.099$. A final difference map showed a general background of about ±0.6 e$^-$/Å^3. The largest peak was 1.09 e$^-$/Å^3, and all peaks greater than 0.7 e$^-$/Å^3 were residuals of lattice species. Final atomic parameters for the tetranuclear cluster and lattice species are listed in Table III, examination of which reveals a wide range of temperature factors and site occupancies for the lattice species. Because these parameters interact strongly in the refinement, they could not be determined with the precision normally associated with a structure at this

(33) Enraf-Nonius Structure Determination Package, Enraf-Nonius, Delft, Holland, 1983.

(34) Main, P.; Fiske, S. J.; Hull, S. E.; Lessinger, L.; Germain, G.; Declercq, J.-P.; Woolfson, M. M. MULTAN 82. A system of Computer Programs for the Automatic Solution of Crystal Structures from X-ray Diffraction Data. Universities of York, England and Louvain, Belgium, 1982.

(35) Churchill, M. R. *Inorg. Chem.* **1973**, *12*, 1213.

Table III. Fractional Atomic Coordinates and Equivalent Isotropic Thermal Parameters for **1**

	x	*y*	*z*	B_{eq} (Å^2)	*M*[b]
Fe(1)	0.2855 (1)	0.1237 (1)	0.8706 (1)	2.96 (3)	
Fe(2)	0.4067 (1)	−0.1660 (1)	0.9666 (1)	3.24 (3)	
O(1)	0.2262 (6)	0.1872 (6)	1.0150 (6)	4.8 (2)	
O(2)	0.0719 (8)	0.3068 (7)	1.0406 (8)	7.5 (3)	
O(3)	0.2527 (6)	0.0874 (6)	0.6778 (6)	4.6 (2)	
O(4)	0.1119 (9)	0.0926 (9)	0.4629 (8)	9.9 (4)	
O(5)	0.2705 (5)	−0.0266 (4)	0.8982 (6)	3.0 (2)	
O(6)	0.3782 (6)	−0.1825 (6)	1.1362 (6)	4.5 (2)	
O(7)	0.3069 (8)	−0.2853 (7)	1.2278 (8)	7.1 (3)	
O(8)	0.3760 (6)	−0.1972 (5)	0.7741 (6)	4.3 (2)	
O(9)	0.2769 (8)	−0.2817 (7)	0.5878 (7)	7.0 (3)	
O(10)	0.2844 (6)	0.2696 (5)	0.8223 (7)	5.0 (2)	
O(11)	0.5301 (6)	−0.3059 (5)	1.0193 (7)	4.7 (2)	
O(12)	0.6827 (8)	−0.4294 (6)	1.154 (1)	9.3 (4)	
O(13)	0.4623 (6)	0.0919 (5)	0.9637 (8)	5.2 (2)	
N(1)	0.0725 (6)	0.1459 (6)	0.7699 (7)	3.2 (2)	
N(2)	0.2315 (6)	−0.2338 (6)	0.8910 (7)	3.4 (2)	
C(1)	0.110 (1)	0.2464 (8)	0.968 (1)	5.0 (3)	
C(2)	0.0241 (9)	0.2380 (8)	0.827 (1)	4.7 (3)	
C(3)	0.031 (1)	0.154 (1)	0.623 (1)	5.8 (4)	
C(4)	0.139 (1)	0.109 (1)	0.582 (1)	5.8 (3)	
C(5)	0.0465 (8)	0.0501 (7)	0.801 (1)	3.8 (3)	
C(6)	0.1461 (8)	−0.0464 (7)	0.816 (1)	3.6 (3)	
C(7)	0.1244 (8)	−0.1403 (7)	0.864 (1)	3.8 (3)	
C(8)	0.313 (1)	−0.2531 (9)	1.129 (1)	5.0 (3)	
C(9)	0.2449 (9)	−0.3030 (8)	0.996 (1)	4.4 (3)	
C(10)	0.2203 (9)	−0.2892 (8)	0.764 (1)	4.4 (3)	
C(11)	0.2940 (9)	−0.2531 (9)	0.701 (1)	4.6 (3)	
C(12)	0.3569 (9)	0.3346 (8)	0.884 (1)	4.8 (3)	
Na(1)	0.000	0.500	1.000	10.0 (3)	
O(14)	0.4918 (8)	−0.5196 (7)	1.1642 (8)	7.4 (3)	
O(15)	−0.0671 (8)	0.4991 (7)	1.1799 (9)	8.6 (3)	
Na(2)	0.568 (2)	−0.128 (2)	0.563 (2)	8.3 (6)*[a]	0.25
Na(3)	0.303 (2)	0.039 (2)	0.415 (2)	21.6 (9)*	0.55
Na(4)	0.476 (3)	−0.568 (3)	1.374 (3)	22 (1)*	0.40
Na(5)	0.317 (2)	0.378 (2)	0.400 (2)	6.9 (6)*	0.20
Na(6)	0.611 (3)	0.221 (3)	0.536 (3)	12.0 (9)*	0.25
Na(7)	0.481 (4)	0.044 (3)	0.471 (4)	8 (1)*	0.15
O(16)	0.213 (1)	−0.485 (1)	1.198 (1)	11.9 (4)*	
O(17)	0.330 (2)	−0.127 (1)	1.447 (2)	13.9 (6)*	0.75
O(18)	0.606 (1)	−0.272 (1)	0.744 (1)	11.1 (4)*	0.80
O(19)	0.835 (2)	0.452 (1)	0.553 (2)	17.5 (6)*	
O(20)	0.222 (2)	0.025 (2)	1.186 (2)	8.4 (5)*	0.50
O(21)	0.139 (2)	0.291 (2)	0.315 (2)	16.1 (6)*	0.80
O(22)	0.401 (2)	0.221 (2)	1.583 (2)	16.9 (8)*	0.70
O(23)	0.127 (2)	0.378 (2)	0.561 (2)	18.2 (8)*	0.70
O(24)	0.503 (2)	−0.013 (2)	0.673 (3)	20 (1)*	0.70
O(25)	0.463 (2)	0.099 (2)	0.636 (3)	6.7 (7)*	0.30
O(26)	0.420 (2)	0.217 (2)	0.445 (3)	3.8 (7)*	0.20
O(27)	0.462 (3)	0.410 (2)	0.561 (3)	16 (1)*	0.50

[a] Asterisked atoms were refined isotropically. [b] M = atom multiplier for partially occupied sites.

level of refinement. We conclude that, within the limits of error associated with elemental analyses, density measurements and crystallographic refinement involving disordered sites, the unit cell contents are best given as $Na_6Fe_4L_2(O)_2(CO_3)_2 \cdot \approx 20H_2O$. Views of the cluster and the $Fe_4N_4O_{16}$ core are shown in Figures 1 and 2, respectively. Lists of anisotropic thermal parameters, H atom parameters, and calculated and observed structure factors are available.[36]

3. Magnetic Measurements. Variable-temperature (15–300 K) magnetic susceptibility data were collected with a VTS-50 SQUID-type susceptometer (S.H.E. Corp.) interfaced with an Apple IIe computer. A cylindrically shaped susceptometer cell with an inner diameter of 4 mm and a threaded air-tight cap was constructed of Delrin for handling this sample. The sample was removed from mother liquor, blotted dry, and then quickly loaded into the cell. The sample weight corresponds to the difference in weights between the loaded and empty cell. A background correction was obtained by measuring the magnetic susceptibility of the empty cell as a function of temperature. Measurements were made at 10 kG. Temperature control and measurement were achieved with the S.H.E. digital temperature control unit, working in conjunction with the computer program CONTROL. Magnetic susceptibility data for $CuSO_4 \cdot 5H_2O$ were measured to check the calibration of the susceptometer. A diamagnetic correction of -750×10^{-6} cgsu was calculated from Pascal's constants.[37] This correction was used to calculate values of the molar paramagnetic susceptibility from the experimental data. The molar paramagnetic susceptibility data were then least-squares fit to the theoretical equation below by means of a computer program. The molar paramagnetic susceptibility of **1** is given as

$$\chi_M = (P/Q)2Ng^2\beta^2/k(T-\theta) + \text{TIP} + \chi_{para}$$

where $\theta = 2J'(P/Q)$, $P = 2e^A + 10e^B + 28e^C + 60e^D + 110e^E$, $Q = 1 + 3e^A + 5e^B + 7e^C + 9e^D + 11e^E$, $A = 2J/kT$, $B = 6J/kT$, $C = 12J/kT$, $D = 20J/kT$, $E = 30J/kT$, TIP = temperature independent paramagnetism, and $\chi_{para} = (PAR)(S)(S+1)(Ng^2\beta^2/3kT)$. This last term accounts for the spin-only magnetism associated with a paramagnetic impurity of mole percentage (PAR) and spin *S*.

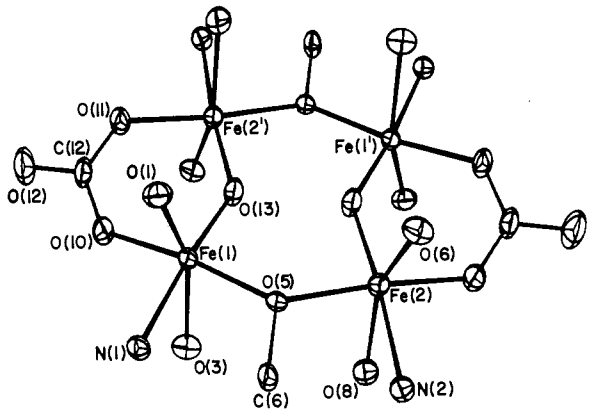

Figure 2. ORTEP view of the $Fe_4N_4O_{16}$ core in **1** showing the bridging oxide and carbonate groups.

Description of the Structure

The structure consists of centrosymmetric tetranuclear complexes (Figure 1) linked by an extensive network involving the lattice Na^+ ions and H_2O molecules. As shown by the bond distances and angles in Table IV, all of the water molecules [O(14) through O(27)] are involved in hydrogen bonding either to each other or to the carboxylate and carbonate O atoms of the tetranuclear clusters. Sodium ions are bonded to water molecules and to the carboxylate O atoms [O(2), O(4), O(7), O(9)] not bonded to Fe. Except for Na(1), the sodium ions are located on partially occupied sites and their coordination geometries are relatively poorly defined. In contrast, the coordination geometry of Na(1), which is located on a center of symmetry, is that of a distorted octahedron formed by bonding to two water molecules [O(15), O(16)] and the carboxylate O atom O(2). Within the distorted octahedron, Na–O contacts and O–Na–O angles range from 2.427 (6) to 2.526 (8) Å and 82.0 (2) to 98.0 (2)°, respectively. These parameters are not unusual for pseudo-octahedrally coordinated sodium.[38] In addition to providing electrostatic stabilization, Na(1) also joins the tetranuclear units via strictly linear O(2)–Na(1)–O(2′) bonds to form infinite Na–(Fe_4)–Na chains along [110].

In the centrosymmetric anions, the asymmetric unit consists of the $Fe_2L(O)CO_3$ group designated by the unprimed atoms in Figure 1. Details of the bridging within the tetranuclear complex are more clearly revealed when most of the ligand nondonor atoms are omitted (Figure 2). Within the asymmetric unit, Fe(1) and Fe(2) are structurally similar although crystallographically unique. Each Fe has a similar NO_5 distorted octahedral ligand donor set in which the O-donors are supplied by two nonbridging acetates [O(1), O(3)], a bridging oxide [O(13)], a bridging alkoxide [O(5)], and a bridging bidentate carbonate [O(10,11)]. While a number of carbonate complexes are known with monodentate,[39]

(36) Supplementary material.

(37) Hatfield, W. E. *Theory and Applications of Molecular Paramagnetism*; Boudreaux, E. A., Mulay, L. N., Eds.; Wiley: New York, 1976; pp 491–495.

(38) Petrikowski, G.; Breitinger, D. K. *Acta Crystallogr.* **1985**, *C41*, 522.

(39) Harlow, R. L.; Simonsen, S. H. *Acta Crystallogr.* **1976**, *B32*, 466. Freeman, H. C.; Robinson, G. *J. Chem. Soc.* **1965**, 3194.

Table IV. Selected Bond Distances (Å) and Angles (deg) in **1**

Distances in the Tetranuclear Complex

Fe(1)–O(1)	2.052 (5)	O(7)–C(8)	1.230 (8)	Na(1)–O(2)	2.463 (6)
Fe(1)–O(3)	2.020 (5)	O(8)–C(11)	1.275 (8)	Na(1)–O(15)	2.427 (6)
Fe(1)–O(5)	2.040 (4)	O(9)–C(11)	1.214 (8)	Na(1)–O(16)	2.526 (8)
Fe(1)–O(10)	1.989 (4)	O(10)–C(12)	1.266 (8)	Na(3)–O(4)	2.47 (2)
Fe(1)–O(13)	1.828 (4)	O(11)–C(12)	1.276 (8)	Na(4)–O(9)	3.00 (2)
Fe(1)–N(1)	2.202 (5)	O(12)–C(12)	1.244 (8)	Na(6)–O(7)	2.49 (2)
Fe(2)–O(5)	2.066 (4)	N(1)–C(2)	1.429 (8)	Na(6)–O(9)	2.53 (2)
Fe(2)–O(6)	2.064 (5)	N(1)–C(3)	1.476 (9)		
Fe(2)–O(8)	2.009 (5)	N(1)–C(5)	1.435 (8)		
Fe(2)–O(11′)	1.997 (4)[a]	N(2)–C(7)	1.482 (7)		
Fe(2)–O(13′)	1.830 (4)	N(2)–C(9)	1.446 (8)		
Fe(2)–N(2)	2.199 (5)	N(2)–C(10)	1.485 (8)		
O(1)–C(1)	1.300 (8)	C(1)–C(2)	1.450 (10)		
O(2)–C(1)	1.232 (8)	C(3)–C(4)	1.501 (11)		
O(3)–C(4)	1.269 (8)	C(5)–C(6)	1.478 (8)		
O(4)–C(4)	1.223 (9)	C(6)–C(7)	1.468 (8)		
O(5)–C(6)	1.406 (6)	C(8)–C(9)	1.494 (10)		
O(6)–C(8)	1.284 (9)	C(10)–C(11)	1.480 (10)		

Possible Hydrogen Bonding Distances (<3 Å)[b]

O(1)···O(18)[i]	2.83 (1)	O(11)···O(14)[iv]	2.892 (7)
O(1)···O(20)	2.93 (1)	O(12)···O(14)	2.780 (9)
O(2)···O(21)[ii]	2.78 (1)	O(12)···O(15)[v]	2.769 (9)
O(3)···O(24)	2.96 (2)	O(17)···O(24)[ii]	2.97 (2)
O(3)···O(25)	2.73 (2)	O(19)···O(23)[vi]	2.80 (2)
O(6)···O(25)[i]	2.70 (2)	O(20)···O(24)[i]	2.88 (2)
O(7)···O(16)	2.96 (1)	O(21)···O(23)	2.90 (2)
O(7)···O(17)	3.00 (1)	O(21)···O(26)	2.91 (2)
O(7)···O(27)[i]	2.91 (2)	O(22)···O(27)[ii]	2.73 (3)
O(8)···O(18)	2.81 (1)	O(24)···O(26)[iii]	2.99 (3)
O(9)···O(19)[iii]	2.81 (1)	O(26)···O(27)	2.76 (3)
O(10)···O(23)	2.90 (2)		

Angles in the Tetranuclear Complex

O(1)–Fe(1)–O(3)	152.6 (2)	O(11′)–Fe(2)–O(13′)	92.8 (2)	O(1)–C(1)–C(2)	117.8 (7)
O(1)–Fe(1)–O(5)	94.4 (2)	O(11′)–Fe(2)–N(2)	94.8 (2)	O(2)–C(1)–C(2)	119.7 (7)
O(1)–Fe(1)–O(10)	88.6 (2)	O(13′)–Fe(2)–N(2)	171.1 (2)	N(1)–C(2)–C(1)	111.1 (6)
O(1)–Fe(1)–O(13)	103.4 (2)	Fe(1)–O(1)–C(1)	115.3 (5)	N(1)–C(3)–C(4)	113.2 (6)
O(1)–Fe(1)–N(1)	75.1 (2)	Fe(1)–O(3)–C(4)	120.6 (5)	O(3)–C(4)–O(4)	124.5 (9)
O(3)–Fe(1)–O(5)	88.3 (2)	Fe(1)–O(5)–Fe(2)	132.3 (2)	O(3)–C(4)–C(3)	116.5 (7)
O(3)–Fe(1)–O(10)	86.4 (2)	Fe(1)–O(5)–C(6)	112.5 (3)	O(4)–C(4)–C(3)	119.0 (8)
O(3)–Fe(1)–O(13)	103.7 (2)	Fe(2)–O(5)–C(6)	111.4 (3)	N(1)–C(5)–C(6)	115.3 (5)
O(3)–Fe(1)–N(1)	78.4 (2)	Fe(2)–O(6)–C(8)	115.0 (5)	O(5)–C(6)–C(5)	110.1 (5)
O(5)–Fe(1)–O(10)	173.5 (2)	Fe(2)–O(8)–C(11)	121.1 (5)	O(5)–C(6)–C(7)	111.8 (5)
O(5)–Fe(1)–O(13)	92.2 (2)	Fe(1)–O(10)–C(12)	132.1 (5)	C(5)–C(6)–C(7)	113.8 (6)
O(5)–Fe(1)–N(1)	81.6 (2)	Fe(2)–O(11′)–C(12′)	132.3 (4)	N(2)–C(7)–C(6)	113.0 (5)
O(10)–Fe(1)–O(13)	92.8 (2)	Fe(1)–O(13)–Fe(2′)	136.4 (3)	O(6)–C(8)–O(7)	122.7 (7)
O(10)–Fe(1)–N(1)	93.6 (2)	Fe(1)–N(1)–C(2)	106.3 (4)	O(6)–C(8)–C(9)	120.3 (7)
O(13)–Fe(1)–N(1)	173.4 (2)	Fe(1)–N(1)–C(3)	107.4 (4)	O(7)–C(8)–C(9)	117.0 (8)
O(5)–Fe(2)–O(6)	94.9 (2)	Fe(1)–N(1)–C(5)	104.4 (4)	N(2)–C(9)–C(8)	107.0 (6)
O(5)–Fe(2)–O(8)	88.8 (2)	C(2)–N(1)–C(3)	115.1 (6)	N(2)–C(10)–C(11)	113.4 (6)
O(5)–Fe(2)–O(11′)	175.5 (2)	C(2)–N(1)–C(5)	113.4 (5)	O(8)–C(11)–O(9)	124.9 (8)
O(5)–Fe(2)–O(13′)	90.6 (2)	C(3)–N(1)–C(5)	109.4 (5)	O(8)–C(11)–C(10)	116.2 (7)
O(5)–Fe(2)–N(2)	82.0 (2)	Fe(2)–N(2)–C(7)	104.2 (3)	O(9)–C(11)–C(10)	118.8 (7)
O(6)–Fe(2)–O(8)	152.6 (2)	Fe(2)–N(2)–C(9)	107.9 (4)	O(10)–C(12)–O(11)	122.5 (6)
O(6)–Fe(2)–O(11′)	87.3 (2)	Fe(2)–N(2)–C(10)	107.1 (4)	O(10)–C(12)–O(12)	118.4 (7)
O(6)–Fe(2)–O(13′)	100.4 (2)	C(7)–N(2)–C(9)	111.8 (5)	O(11)–C(12)–O(12)	119.1 (7)
O(6)–Fe(2)–N(2)	75.5 (2)	C(7)–N(2)–C(10)	111.7 (5)	O(2)–Na(1)–O(15)	85.8 (2)
O(8)–Fe(2)–O(11′)	87.5 (2)	C(9)–N(2)–C(10)	113.5 (5)	O(2)–Na(1)–O(16)	86.4 (2)
O(8)–Fe(2)–O(13′)	106.7 (2)	O(1)–C(1)–O(2)	122.5 (8)	O(15)–Na(1)–O(16)	82.0 (2)
O(8)–Fe(2)–N(2)	78.2 (2)				

[a] Primed atoms are related to unprimed atoms by $1-x, -y, 2-z$. [b] Symmetry transformations: i = $1-x, -y, 2-z$; ii = $x, y, 1+z$; iii = $1-x, -y, 1-z$; iv = $1-x, -1-y, 2-z$; v = $1+x, y-1, z$; vi = $1-x, 1-y, 1-z$.

chelating,[40] or bridging[41,42] geometries, to our knowledge, the title complex provides the first structurally characterized bridging carbonate of Fe.

The bent Fe_2O(oxo) unit [Fe(1)–O(13)–Fe(2), 136.4 (3)°] contains the shortest of the Fe–O bonds [1.828 (4), 1.830 (4) Å]. These are equivalent within experimental error and fall at the upper end of the range reported (1.76–1.82 Å) for other oxo-bridged Fe(III) dimers,[3] including the hemerythrin models which contain carboxylate[12,13] or phosphodiester[23] bridges in addition to the oxo-bridge. In contrast, the Fe–O–Fe angle lies near the lower end of the range reported (139–180°) for Fe_2O(oxo) complexes, yet is substantially larger than that found (103–111°) for hydroxo/alkoxo-bridged Fe(III) dimers.[3] Thus, the structural parameters of the Fe(1)–O(13)–Fe(2) unit mitigate against hydroxy bridging, as does the relatively large value of the coupling constant J [−63.4 cm^{-1} compared with −7.3 to −17.1 cm^{-1} for hydroxo/alkoxo-bridged dimers[3]]. Finally, we note that the bridging atom O(13) lies near the center of the anion and is not

(40) Churchill, M. R.; Harris, G. M.; Lashewycz, R. A.; Dasgupta, T. P.; Koshy, K. *Inorg. Chem.* **1979**, *18*, 2290.
(41) Gagne, R. R.; Gall, R. S.; Lisensky, G. C.; Marsh, R. E.; Speltz, L. M. *Inorg. Chem.* **1979**, *18*, 771.
(42) Kolks, G.; Lippard, S. J.; Waszczak, J. V. *J. Am. Chem. Soc.* **1980**, *102*, 4832 and references cited therein.

Table V. Temperature Dependence of the Observed and Calculated Magnetic Susceptibility and Magnetic Moments of $Na_6(\mathbf{1})\cdot\sim 20H_2O$

	susceptibility		magnetic moment	
temp	exptl	calcd[a]	exptl	calcd
10.0	0.00690	0.00711	0.371	0.377
20.0	0.00551	0.00488	0.469	0.442
24.2	0.00481	0.00468	0.483	0.476
30.0	0.00444	0.00480	0.516	0.536
34.0	0.00460	0.00506	0.559	0.587
38.0	0.00520	0.00542	0.628	0.642
40.0	0.00616	0.00562	0.702	0.671
50.0	0.00722	0.00668	0.850	0.817
60.0	0.00793	0.00762	0.976	0.956
69.9	0.00849	0.00835	1.089	1.080
80.6	0.00895	0.00895	1.201	1.201
89.0	0.00929	0.00935	1.292	1.297
101.3	0.00963	0.00974	1.397	1.405
110.4	0.00987	0.01000	1.476	1.485
120.4	0.01011	0.01024	1.560	1.571
130.5	0.01033	0.01045	1.642	1.651
140.0	0.01051	0.01062	1.715	1.724
150.0	0.01069	0.01078	1.791	1.798
160.8	0.01087	0.01094	1.870	1.875
170.8	0.01104	0.01106	1.941	1.943
180.7	0.01117	0.01118	2.009	2.010
190.7	0.01131	0.01129	2.077	2.075
200.1	0.01141	0.01138	2.137	2.133
209.8	0.01151	0.01147	2.197	2.193
220.4	0.01160	0.01156	2.261	2.257
230.0	0.01168	0.01163	2.317	2.313
240.0	0.01176	0.01171	2.376	2.370
249.8	0.01183	0.01178	2.431	2.426
259.8	0.01190	0.01184	2.486	2.480

[a] Calculated values were obtained by the expressions given in the text for $g = 2.0$, $J = -63.4$ cm^{-1}, $J' = -11.2$ cm^{-1}, and TIP = 800×10^{-6} cgsu.

within (hydrogen) bonding distance of any *lattice* species. However, the O(13)···O(13′) distance (2.408 (9) Å) is such that the presence of an H^+ ion at or near the the center of symmetry is possible and cannot be ruled out solely on crystallographic grounds owing in part to the lattice disorder problems. The presence of such an H^+ ion would confer partial hydroxo character to the O(13), O(13′) oxo groups and would be expected to result in elongation of the Fe–O(oxo) distances along with attenuation of the superexchange coupling via the O(13,13′) groups. An additional H^+ ion would overaccount for the possibly missing ≈0.5 Na^+ ion determined from elemental analysis (Table I) but would be consistent with the number of Na^+ ions (≈4.6) located crystallographically.

The Fe–N bonds [2.202 (5), 2.199 (5) Å] are equivalent, and possibly lengthened somewhat due to a trans influence from the strong Fe–O(oxo) bond.[13] The Fe–O(alkoxo) bonds [2.040 (4), 2.066 (4) Å] are nearly equivalent and fall outside the range [1.93–2.01 Å] reported for various $Fe_2(OR)_2^{4+}$ (R = H, alkyl) dimers[3,4] and the sole example of a Fe–OH–Fe dimer (which contains additional bridging by two acetate groups).[15] Moreover, the Fe(1)–O(5)–Fe(2) bridging angle in the tetranuclear unit (132.3 (2)°) is larger than those reported for the dimers with either two bridges (103–110.6°) or a single bridge (123.1°).

The bridging carbonate group results in equivalent Fe–O bond lengths of 1.989 (4) and 1.997 (4) Å. Within the bidentate carbonate unit, the terminal C(12)–O(12) bond [1.244 (8) Å] is 0.02–0.03 Å shorter than the bonds from C(12) to the ligating oxygen atoms O(10,11) [1.266 (8), 1.276 (8) Å]. In other structures in which a bidentate carbonate was formulated as $O_2C{=}O$,[40,41] the terminal C–O bond was ca. 0.07–0.08 Å shorter than the other two C–O bonds, while for the lone example of a bridging bicarbonate,[43] O_2C–OH, the terminal C–OH bond was 0.06 Å *longer* than the mean of the C–O bonds. In the present structure, the less-than-expected shortening of C(12)–O(12) is consistent with hydrogen bonding to O(12) or partial protonation of O(12) by the H atoms of the lattice water molecules O(14) and O(15) (Table IV). Lastly, the structural parameters observed for the tetraacetate ligand are typical and will not be considered further.

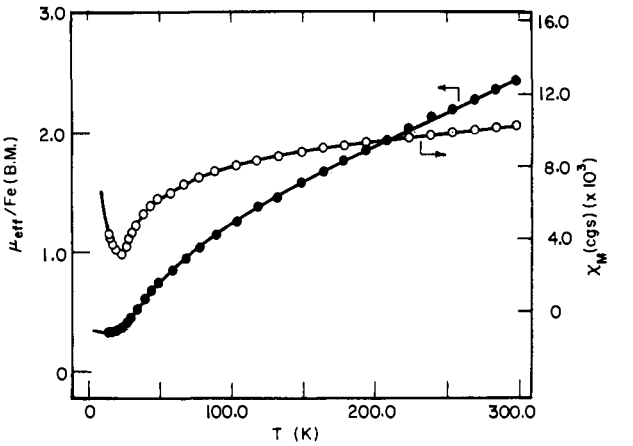

Figure 3. Temperature dependence of the paramagnetic susceptibility per Fe(III) and magnetic moment per Fe(III) for the tetranuclear complex **1**. Circles represent experimental data and the solid lines were calculated with use of the molecular field model described in the text.

Magnetic Susceptibility Results and Discussion

The effective magnetic moment per iron ion, μ_{eff}/Fe, in the tetranuclear complex **1** varies gradually from 2.42 μ_B at 300 K down to 0.36 μ_B at 15 K (see Figure 3). The molar paramagnetic susceptibility, χ_M, also decreases gradually as the temperature is lowered and has a minimum value at 25 K. Susceptibility data are available as supplementary material.

On the basis of the general features of superexchange coupling in polynuclear Fe(III) species linked by O-donor ligands, the dominant superexchange pathway in the tetranuclear complex **1** is expected to be via the oxo bridge O(13).[3] We accordingly chose to view the magnetic behavior as that of two oxo/carbonato-bridged Fe(III) binuclear complexes which display intermolecular coupling via the two relatively long alkoxo bridges that join the binuclear species to form the tetranuclear complexes (Figure 2). Intradimer magnetic coupling (J) is expected to be substantially larger than interdimer coupling (J'). Interdimer coupling within the tetranuclear complex was treated by the molecular field approximation[44] by using the equations and procedures described in section 3 of the Experimental Section. Fitting the experimental χ_M data to this molecular field approximation gave $J = -63.4$ cm^{-1}, $J' = -11.2$ cm^{-1}, $g = 2.0$, and TIP = 800×10^{-6} cgsu. The software used to fit the data employs a simplex minimization approach designed to vary the parameters within a reasonably large parameter space to select the most pronounced minimum. The same fit was arrived at even though considerably different values of J and J' were input initially. The increase in χ_M below 25 K could result from the presence of high-spin Fe(III) in the small amount of mother liquor that accompanied the sample. As noted in the Experimental Section, the crystals easily dehydrate and crack. Samples for the susceptibility study were blotted dry immediately before use and placed in a sealed container to prevent dehydration. We believe that the presence of some remaining mother liquor is the cause of the rise in χ_M below 25 K. This effect can be accounted for if approximately 2% of the total iron is present as either monomeric $S = {}^5/_2$ Fe(III) or a weakly coupled (i.e., hydroxo-bridged) Fe(III) dimer. The presence of Fe(III) in the mother liquor would lead to observed Fe analyses higher than those calculated, consistent with the data in Table I. The χ_{para} term (see Experimental Section) corrects for paramagnetic impurities and was used in the least-squares fitting of the mag-

(43) Meanwell, N. J.; Smith, A. J.; Adams, H.; Okeya, S.; Maitlis, P. M. *Organometallics* **1983**, *2*, 1705.

(44) See ref 37, p 400.

netochemical data. The TIP term is somewhat large; we suspect it is an artifact due to the presence of impurities and is, therefore, not very important.

The interdimer coupling obtained from the above analysis (-11.2 cm^{-1}) is typical of the weak antiferromagnetic interactions observed for Fe(III) dimers containing hydroxo or alkoxo bridging.[3,4,15] Although the Fe-OR-Fe bridging angle for the interdimer bridges is large, the extent of superexchange coupling for $^6A_{1g}$ Fe(III) generally appears to be quite insensitive toward variations in bridging angles.[3,4] The intradimer coupling (-63.4 cm^{-1}) is well below the values (-90 to -120 cm^{-1})[3,12] usually observed for oxo-bridged Fe(III) dimers. Owing to the weak antiferromagnetic coupling that carboxylate-bridged Fe(III) systems are thought to exhibit,[3] coupling via the carbonate probably is negligible relative to that via the oxo-bridge. The closest approximation to the "dimer" subunit of the tetranuclear complex **1** is the oxo-bridged Fe(III) binuclear complex with additional phosphodiester bridging that recently has been characterized by Armstrong and Lippard.[23] This latter binuclear complex exhibits typical antiferromagnetic superexchange ($J = -98$ cm^{-1}). The Fe-O(oxo) distances [1.812 (5), 1.804 (5) Å] and Fe-O(oxo)-Fe angle [134.7 (3)°] are close to those observed for the corresponding structural features of **1**. However, additional coordination to the Fe-O-Fe unit can change the coupling constant significantly. Thus, coordination of a third Fe(III) to an Fe_2O core at a distance of 2.067 Å causes the Fe-O(oxo) bond distances to increase (1.862 (7), 1.867 (7) Å) and coupling within the Fe_2O unit to decrease to -55 cm^{-1}.[24] These bond distances and the superexchange coupling are intermediate between those reported for typical oxo-bridged Fe(III) binuclear complexes and oxo-bridged Fe(III) trinuclear complexes [Fe-O = 1.92-1.96 Å, $J \approx -30$ cm^{-1}].[3] The reason for the unexpectedly low intradimer coupling in **1** may be that the Fe-O(oxo) bond distances have elongated just to the point where the superexchange coupling becomes significantly attenuated. The factors responsible for the slight elongation of the Fe-O(oxo) bond distances in **1** cannot be identified with certainty. Possibly, this effect is due to strain within the tetranuclear cluster or to subtle electronic effects associated with the carbonato bridging. Packing of the tetranuclear complex precludes the approach of lattice water to the O(13) and O(13′) atoms, while structural parameters of the Fe_2O(oxo) unit rule out hydroxo-bridging and thus the presence of two protons situated about the center of the cluster between O(13) and O(13′). As noted above, however, we cannot rule out the presence of a single H^+ at (ordered) or near (disordered structure) the center of the cluster. The presence of this H^+ ion would serve to lengthen the Fe-O(oxo) bonds and reduce the extent of antiferromagnetic coupling. The reduced antiferromagnetism ($J \approx -77$ cm^{-1}) reported for oxyhemerythrin presumably is related to the clear H-bonding interaction observed between the hydroperoxide ligand and the oxo-bridge.[10b]

Acknowledgment. Research at Rutgers University was supported by a crystallographic instrumentation grant from the National Institutes of Health (Grant 1510 RRO 1486 01A1), and research at the University of Illinois was supported by National Institutes of Health Grant HL13652.

Registry No. Na_6(**1**)·≈$20H_2O$, 105597-77-1.

Supplementary Material Available: Listing of anisotropic thermal parameters, H atom parameters, and magnetic susceptibility data (3 pages); observed and calculated structure factor tables (16 pages). Ordering information is given on any current masthead page.

Hydride Transfer in the Oxidation of Alcohols by $[(bpy)_2(py)Ru(O)]^{2+}$. A k_H/k_D Kinetic Isotope Effect of 50

Lee Roecker and Thomas J. Meyer*

Contribution from the Department of Chemistry, The University of North Carolina, Chapel Hill, North Carolina 27514. *Received June 2, 1986*

Abstract: The kinetics of oxidation of a series of alcohols by $[(bpy_2(py)Ru^{IV}(O)]^{2+}$ (bpy is 2,2′-bipyridine and py is pyridine) have been studied in aqueous solution and in acetonitrile. The reactions are first order in both alcohol and $Ru^{IV}{=}O^{2+}$, pH independent from pH 1.0 to 6.8, and slightly slower in acetonitrile than in water. Rate constants for oxidation increase with substituent as follows: methyl < primary < secondary < allylic ≲ benzylic. Tertiary alcohols are unreactive, and in the series of para substituted benzylic alcohols, $X\text{-}C_6H_4CH_2OH$ (X = CH_3O, CH_3, H, F, Cl, CF_3, and NO_2), the rate of oxidation is relatively insensitive to the substituent X. In aqueous solution k ranges from (3.5 ± 0.1) × 10^{-4} M^{-1} s^{-1} for the oxidation of methanol ($\Delta H^{\ddagger}$ = 14 ± 2 kcal/mol, $\Delta S^{\ddagger}$ = −26 ± 6 eu) to 2.43 ± 0.03 M^{-1} s^{-1} for the oxidation of benzyl alcohol ($\Delta H^{\ddagger}$ = 5.8 ± 0.4 kcal/mol, $\Delta S^{\ddagger}$ = −38 ± 1 eu). Large C-H kinetic isotope effects are observed, but solvent isotope effects are negligible. For CH_3OH compared to CD_3OH, k_H/k_D = 9 at 25 °C and for benzyl alcohol, $C_6H_5CH_2OH$ compared to $C_6H_5CD_2OH$, k_H/k_D = 50 ± 3 at 25 °C. Spectral evidence, in conjunction with the isotope effect data, suggests that oxidation of alcohols by $[(bpy)_2(py)Ru^{IV}(O)]^{2+}$ occurs by a two-electron, hydride transfer.

Oxidation of a variety of alcohols by oxo complexes of ruthenium have been reported over the past 20 years, but few mechanistic details are known.[1,2] Notable exceptions include the work of Lee and co-workers who have observed a primary kinetic isotope effect of 4.6 (25 °C, 1.94 M $HClO_4$) in the oxidation of 2-propanol to acetone by RuO_4^{2-} and who observe the formation of cyclobutanone from the oxidation of cyclobutanol by RuO_4 and RuO_4^{2-} suggestive of a two-electron, hydride transfer oxidation pathway.[3,4] An attractive feature associated with reagents like RuO_4 is that

(1) Lee, D. G.; van den Engh, M. In *Oxidation in Organic Chemistry, Part B*; Trahanovsky, W. S., E.; Academic Press: New York, 1973.
(2) Gagne, R. R.; Marks, D. N. *Inorg. Chem.* **1984**, *23*, 65 and references therein.
(3) Lee, D. G.; van den Engh, M. *Can. J. Chem.* **1972**, *50*, 2000.
(4) Lee, D. G.; Spitzer, U. A.; Cleland, J.; Olson, M. E. *Can. J. Chem.* **1976**, *54*, 2124.

0002-7863/87/1509-0746$01.50/0